

Performance Analysis of Downlink MIMO-NOMA Systems over Weibull Fading Channels

*Note: This work has been submitted to the IEEE for possible publication.

Copyright may be transferred without notice, after which this version may no longer be accessible.

Lenin Patricio Jiménez Jiménez
Dept. of Communications
University of Campinas
Campinas, Brazil
l264366@dac.unicamp.br

Fernando Darío Almeida García
Dept. of Communications
University of Campinas
Campinas, Brazil
ferdardal@decom.fee.unicamp.br

Maria Cecilia Luna Alvarado
Dept. of Communications
University of Campinas
Campinas, Brazil
m264371@dac.unicamp.br

Gustavo Fraidenraich
Dept. of Communications
University of Campinas
Campinas, Brazil
gf@decom.fee.unicamp.br

Michel Daoud Yacoub
Dept. of Communications
University of Campinas
Campinas, Brazil
mdyacoub@unicamp.br

José Cândido S. Santos Filho
Dept. of Communications
University of Campinas
Campinas, Brazil
candido@decom.fee.unicamp.br

Eduardo Rodrigues de Lima
Hardware Dept.
Eldorado Research Institute
Campinas, Brazil
eduardo.lima@eldorado.org.br

Abstract—This work analyzes the performance of a downlink multiple-input multiple-output (MIMO) non-orthogonal multiple access (NOMA) multi-user communications system. To reduce hardware complexity and exploit antenna diversity, we consider a transmit antenna selection (TAS) scheme and equal-gain combining (EGC) receivers operating over independent and identically distributed (i.i.d.) Weibull fading channels. Performance metrics such as the outage probability (OP) and the average bit error rate (ABER) are derived in an exact manner. An asymptotic analysis for the OP and for the ABER is also carried out. Moreover, we obtain exact expressions for the probability density function (PDF) and the cumulative distribution function (CDF) of the end-to-end signal-to-noise ratio (SNR). Interestingly, our results indicate that, except for the first user (nearest user), in a high-SNR regime the ABER achieves a performance floor that depends solely on the user's power allocation coefficient and on the type of modulation, and not on the channel statistics or the amount of transmit and receive antennas. To the best of the authors' knowledge, no performance analyses have been reported in the literature for the considered scenario. The validity of all our expressions is confirmed via Monte-Carlo simulations.

Index Terms—Non-orthogonal multiple access (NOMA), multiple-input multiple-output (MIMO), transmit antenna selection (TAS), equal-gain combining (EGC), Weibull fading, average bit error rate (ABER), outage probability (OP).

I. INTRODUCTION

The constant demand for massive connectivity scenarios in the sixth-generation (6G) network systems poses greater challenges than technologies such as orthogonal multiple access (OMA) can manage [1], [2]. In view of this, researchers have proposed several techniques with the potential of meeting the requirements of advanced wireless networks,

such as 6G. Among them, we highlight the non-orthogonal multiple access (NOMA) technique since it (i) significantly improves spectral and energy efficiency, (ii) provides ultra-reliable and low-latency communications (URLLC), and (iii) enables massive connectivity [3]–[8]. NOMA can be classified into two schemes: code-domain and power-domain multiplexing. In this paper, we will focus on the latter, although the same framework can be applied to the former with no substantial adjustments. The difference between NOMA and its predecessor, OMA, is that NOMA allocates time-frequency resources that are superposed and transmitted to multiple users, where for each user a specific power coefficient is allocated based on their channel conditions. On the other hand, OMA allocates resources to each user either in time, in frequency, or in code [9]. In NOMA, each receiver can decode its own information by using the method of successive interference cancellation (SIC) [3], [10], [11].

To explore power consumption reduction as well as hardware complexity and, at the same time, to improve system capacity, several works analyzed the performance of a NOMA system over different antenna configurations, e.g., single-input single-output (SISO), multiple-input single-output (MISO), single-input multiple-output (SIMO), and multiple-input multiple-output (MIMO). For instance, in [12], the authors carried out an outage probability (OP) analysis for a SISO-NOMA system in a multi-user scenario operating over κ - μ and η - μ fading environments. In [13], the authors derived an approximate closed-form solution for the OP of a SIMO-NOMA system considering equal-gain combining (EGC) receivers operating over κ - μ fading channels and employing the special case when $\kappa \rightarrow 0$ (i.e., the Nakagami- m fading model). The same authors proposed in [14] an approximate analysis

The work of L. P. J. Jiménez was supported by Eldorado Research Institute. The work of F. D. A. García was supported by the São Paulo Research Foundation (FAPESP) under Grant 2021/03923-9.

for the OP considering a SIMO-NOMA system and employing η - μ fading channels, selection combining (SC), maximal-ratio combining (MRC), and EGC receivers. In [15] and [16], an analysis of performance and security for a MIMO-NOMA system using a transmit antenna selection (TAS) scheme and Rayleigh fading was presented. In [17], the authors calculated the OP for a MIMO-NOMA system by means of Monte-Carlo simulations and employing a majority-based TAS (TAS-maj) technique, MRC receivers, and Rayleigh fading. In [18] and [19], the authors derived exact expressions for the OP, the average bit error rate (ABER), and the ergodic capacity (EC) of a SISO-NOMA system in a two-user scenario and considering κ - μ and shadowed κ - μ fading channels, respectively. Recently, in [20], the authors derived exact expressions for the OP, the ABER, and the EC for both a SISO-NOMA and MISO-NOMA (with TAS) system considering independent double Nakagami- m fading channels.

According to what has been shown in the open literature, and to the best of our knowledge, no *exact* performance analysis has been carried out employing NOMA, TAS, and EGC receivers for any of the well-known fading distributions, not even for Rayleigh. This work is the first of its kind analyzing, in an exact manner, the performance of a NOMA system considering the two aforementioned diversity schemes: TAS and EGC receivers. For the analysis, we consider the Weibull fading model as it can accurately describe the non-linearities of the propagation medium in addition to encompassing, as special cases, important fading scenarios such as Rayleigh and exponential models.

The contributions of this work are summarized as follows:

- 1) Novel exact expressions for the probability density function (PDF) and cumulative distribution function (CDF) of the signal-to-noise ratio (SNR) of a MIMO-NOMA system operating over independent and identically distributed (i.i.d.) Weibull fading channels.
- 2) New exact formulations for key performance metrics, namely, OP and ABER. Two important remarks are in order. Due to the versatility of the Weibull fading model, the exact OP and the ABER of MRC receivers can also be found from our analytical findings by replacing k by $k/2$, where k is the shape parameter of the Weibull distribution. Moreover, if we consider a single user (a non-NOMA system) and a single transmitting antenna, then our expressions provide an exact analysis in terms of OP and ABER for a SIMO system over Weibull fading channels, which so far have only been found as approximate, limited, or computationally expensive solutions [21]–[27].
- 3) Asymptotic closed-form expressions for the OP and the ABER. We show that, for the OP, the diversity order equals $(kMN)/2$, where M and N are the number transmit and receive antennas, respectively. In contrast, for the ABER, the diversity order remains $(kMN)/2$ only for the first user, while being nil for the remaining ones, with the corresponding performance floor at high SNR solely depending on the user's power allocation

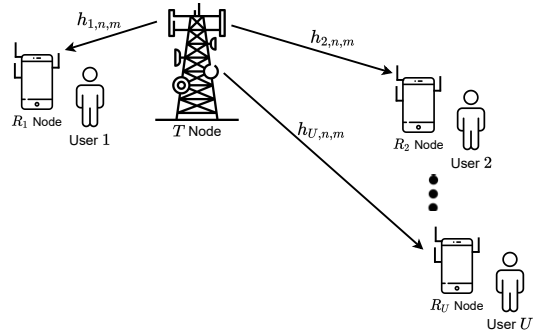


Fig. 1. Downlink MIMO-NOMA system model.

coefficient and the employed modulation.

The remainder of this manuscript is organized as follows. Section II introduces the MIMO-NOMA system model. Section III obtains novel exact expressions for the SNR' statistics. Section IV derives exact and asymptotic expressions for the OP and the ABER. Section V discusses the representative numerical results. Finally, Section VI concludes this paper.

II. SYSTEM MODEL

A downlink NOMA-MIMO system with a single transmitter node T and multiple receiving users R_l ($l \in \{1, 2, \dots, U\}$) is considered, as shown in Fig. 1. The transmitter and receiving nodes are equipped with M and N antennas, respectively. Based on NOMA principle, T simultaneously serves the multiple users over the same time and frequency resources. Users with poor channel conditions are allocated with high power coefficients, and vice-versa. The complex channel coefficient between the m -th transmitting antenna and the n -th receiving antenna of the l -th user is denoted by $h_{l,n,m}$. Herein, we assume that the envelope of each channel coefficient (i.e., $|h_{l,n,m}|$) follows a Weibull distribution with shape and scale parameters k and λ , respectively. Also, we assume that all channels experience i.i.d. fading and that perfect SIC is implemented to decode the superimposed signals [28]. Without loss of generality, we assume that $|h_{U,n,m}| \leq \dots \leq |h_{l,n,m}| \leq \dots \leq |h_{1,n,m}|$.¹ Accordingly, the users' power allocation coefficients can be sorted as $\beta_U \geq \dots \geq \beta_l \geq \dots \geq \beta_1$, obeying $\sum_{j=1}^U \beta_j = 1$.

The superimposed information signal sent by node T is given by $s = \sum_{j=1}^U \sqrt{P_j} x_j$ where x_j is the information sent to each user, $P_j = \beta_j P_s$ is the transmit power, and P_s is the total transmit power. To leverage the benefits of multiple antennas (i.e., to exploit antenna diversity), we employ the TAS strategy at transmission and EGC receivers at reception. Thus, the received signal at the l -th user can be written as

$$y_{l,n,m^*} = h_{l,n,m^*} \sum_{j=1}^U \sqrt{\beta_j P_s} x_j + n_{l,n}, \quad (1)$$

where $n_{l,n}$ is the complex additive white Gaussian noise (AWGN) with zero mean and variance σ_0^2 present at the n -th

¹The decoding order of SIC is given by the channel ordering [29].

antenna of the l -th user, and m^* denotes the single antenna of node T selected for transmission according to the following criterion [30]:

$$m^* = \arg \max_{1 \leq m \leq M} \left(\sum_{n=1}^N |h_{u,n,m}| \right)^2. \quad (2)$$

III. SNR'S STATISTICS

According to (1), the instantaneous SNRs at the first (nearest user) and u -th ($u \in \{2, 3, \dots, U\}$) users are respectively given by

$$\chi_1 = \frac{\beta_1 \rho \Psi_1^2}{N} \quad (3a)$$

$$\chi_u = \frac{\beta_u \rho \Psi_u^2}{N + \rho \Psi_u^2 \vartheta_u}, \quad (3b)$$

where $\rho = P_s/\sigma_0^2$ denotes the transmit SNR, $\vartheta_u = \sum_{j=1}^{u-1} \beta_j$, $\Psi_1 = \sum_{n=1}^N |h_{1,n,m^*}|$, and $\Psi_u = \sum_{n=1}^N |h_{u,n,m^*}|$ with $|h_{u,n,m^*}|$ being the independent and identically distributed (i.i.d.) Weibull fading envelopes satisfying the criterion in (2).

Taking into account that all channels undergo independent fading, the CDF of Ψ_u can be found as

$$F_{\Psi_u}(\psi_u) = \left(\Pr \left[\sum_{n=1}^N |h_{u,n,m^*}| \leq \psi_u \right] \right)^M, \quad (4)$$

where $\Pr[\cdot]$ denotes probability.

Capitalizing on [31, Proposition 1], we can rewrite (4) as

$$F_{\Psi_u}(\psi_u) = \left(\frac{k}{\lambda^k} \right)^{NM} \left(\sum_{i=0}^{\infty} \frac{\delta_i \psi_u^{ik+kN}}{\Gamma(ik + Nk + 1)} \right)^M, \quad (5)$$

where $\Gamma(\cdot)$ is the gamma function [32, eq. (6.1.1)], and the coefficients δ_i can be obtained recursively as

$$\delta_0 = \Gamma(k)^N \quad (6a)$$

$$\delta_i = \frac{1}{i\Gamma(k)} \sum_{p=1}^i \frac{\delta_{i-p}(-i+pN+p)\Gamma(pk+k)\left(-\left(\frac{1}{\lambda}\right)^k\right)^p}{p!}. \quad (6b)$$

From (5), we let

$$\left(\sum_{i=0}^{\infty} \psi_u^{k(i+N)} \eta_i \right)^M = \sum_{i=0}^{\infty} \psi_u^{k(i+N)} \xi_i, \quad (7)$$

in which $\eta_i = \delta_i/\Gamma(ik + Nk + 1)$.

Now, we make use of the following differential equation:

$$\varrho \left(\varrho^M \right)' = M \varrho^M \varrho', \quad (8)$$

where the ‘‘apostrophe’’ denotes derivative with respect to $\psi_u^{k(i+N)}$, and

$$\varrho = \sum_{i=0}^{\infty} \psi_u^{k(i+N)} \eta_i \quad (9)$$

$$\varrho^M = \sum_{i=0}^{\infty} \psi_u^{k(i+N)} \xi_i. \quad (10)$$

After solving (8), the coefficients ξ_i can be calculated as

$$\xi_0 = \left(\frac{\delta_0}{\Gamma(kN+1)} \right)^M \quad (11a)$$

$$\xi_i = \frac{\Gamma(kN+1)}{i\delta_0} \sum_{q=1}^i \frac{(-i+qM+q)\delta_i \xi_{i-q}}{\Gamma(qk+Nk+1)}, \quad i \geq 1. \quad (11b)$$

Finally, replacing (7) and (11) into (5), we can respectively express the CDF and PDF of Ψ_u as follows:

$$F_{\Psi_u}(\psi_u) = \left(\frac{k}{\lambda^k} \right)^{NM} \sum_{i=0}^{\infty} \xi_i \psi_u^{k(i+NM)} \quad (12)$$

$$f_{\Psi_u}(\psi_u) = \frac{k^{NM+1}}{\psi_u} \left(\frac{\psi_u}{\lambda} \right)^{kNM} \sum_{i=0}^{\infty} \xi_i (i+NM) \psi_u^{ik}. \quad (13)$$

Using (3b), the CDF of χ_u can be found as

$$\begin{aligned} F_{\chi_u}(\chi_u) &= \Pr \left[\Psi_u \leq \sqrt{\frac{N\chi_u}{\rho(\beta_u - \chi_u \vartheta_u)}} \right] \\ &= F_{\Psi_u} \left(\sqrt{\frac{N\chi_u}{\rho(\beta_u - \chi_u \vartheta_u)}} \right). \end{aligned} \quad (14)$$

Then, by employing (12) and (14), the CDF of χ_u can be finally expressed as

$$F_{\chi_u}(\chi_u) = \left(\frac{k}{\lambda^k} \right)^{NM} \sum_{i=0}^{\infty} \xi_i \left(\frac{N\chi_u}{\rho(\beta_u - \chi_u \vartheta_u)} \right)^{\frac{k}{2}(i+NM)}. \quad (15)$$

After differentiating (15) with respect to χ_u , the PDF of χ_u can be found as

$$\begin{aligned} f_{\chi_u}(\chi_u) &= \frac{\beta_u k^{1+NM}}{2\chi_u(\beta_u - \chi_u \vartheta_u)} \left(\frac{1}{\lambda} \right)^{kNM} \\ &\quad \times \sum_{i=0}^{\infty} \xi_i (i+MN) \left(\frac{N\chi_u}{\rho(\beta_u - \chi_u \vartheta_u)} \right)^{\frac{k}{2}(i+NM)}. \end{aligned} \quad (16)$$

Following a similar approach as in (15) and (16), the CDF and PDF of the SNR at the first user can be respectively found as

$$F_{\chi_1}(\chi_1) = \left(\frac{k}{\lambda^k} \right)^{MN} \sum_{i=0}^{\infty} \xi_i \left(\frac{N\chi_1}{\beta_1 \rho} \right)^{\frac{k}{2}(i+MN)} \quad (17a)$$

$$f_{\chi_1}(\chi_1) = \frac{k^{MN+1}}{2\chi_1 \lambda^{kMN}} \sum_{i=0}^{\infty} \xi_i (i+MN) \left(\frac{N\chi_1}{\beta_1 \rho} \right)^{\frac{k}{2}(i+MN)}. \quad (17b)$$

IV. PERFORMANCE ANALYSIS

In this section, we use our derived formulations to analyze the performance of an EGC receiver subject to Weibull fading.

A. Outage Probability

The OPs for the first and u -th users are respectively defined as the probability that χ_1 and χ_u fall below a specified threshold, i.e.,

$$P_{\text{out},\nu} \triangleq \Pr[\chi_\nu \leq \gamma_\nu] = F_{\chi_\nu}(\gamma_\nu), \quad (18)$$

where $\nu \in \{1, u\}$ denotes the associated user (recall that $u \in \{2, 3, \dots, U\}$).

Now, from (15) and (18), the OPs for the first and u -th users are respectively given by

$$P_{\text{out},1} = \left(\frac{k}{\lambda^k}\right)^{NM} \sum_{i=0}^{\infty} \xi_i \left(\frac{N\gamma_1}{\rho\beta_1}\right)^{\frac{k}{2}(i+NM)} \quad (19)$$

$$P_{\text{out},u} = \left(\frac{k}{\lambda^k}\right)^{NM} \sum_{i=0}^{\infty} \xi_i \left(\frac{N\gamma_u}{\rho(\beta_u - \gamma_u \vartheta_u)}\right)^{\frac{k}{2}(i+NM)} \quad (20)$$

Moreover, we analyze the system performance in a high SNR regime (i.e., when $\rho \rightarrow \infty$). Then, since the first term dominates the series in (19) and (20) (i.e., the term associated with $i = 0$), the asymptotic OPs for the first and u -th users can be expressed as

$$P_{\text{out},\nu} \simeq (O_{c,\nu} \rho)^{-O_{d,\nu}}, \quad (21)$$

where \simeq denotes ‘‘asymptotically equal to’’; $O_{d,1} = kMN/2$ and $O_{d,u} = kMN/2$ are the diversity gains for the first and u -th users, respectively; and

$$O_{c,1} = \frac{\lambda^2 \beta_1}{N\gamma_1} \left(\frac{\Gamma(k+1)^N}{\Gamma(kN+1)}\right)^{-\frac{2}{kN}} \quad (22)$$

$$O_{c,u} = \frac{\lambda^2 (\beta_u - \gamma_u \vartheta_u)}{N\gamma_u} \left(\frac{\Gamma(k+1)^N}{\Gamma(kN+1)}\right)^{-\frac{2}{kN}} \quad (23)$$

are the coding gains for the first and u -th users, respectively.

B. ABER

The ABERs for a pre-detection EGC receiver for the first and u -th users are respectively given by [33, eq. (9.61)]

$$P_{b,1} = \frac{1}{2} \int_0^{\infty} \text{erfc} \left(\sqrt{\frac{\mathcal{A} \beta_1 \rho \psi_1^2}{N}} \right) f_{\Psi_1}(\psi_1) d\psi_1 \quad (24)$$

$$P_{b,u} = \frac{1}{2} \int_0^{\infty} \text{erfc} \left(\sqrt{\frac{\mathcal{A} \beta_u \rho \psi_u^2}{N + \rho \psi_u^2 \vartheta_u}} \right) f_{\Psi_u}(\psi_u) d\psi_u, \quad (25)$$

in which $\text{erfc}(\cdot)$ is the complementary error function [32, eq. (7.1.2)], and \mathcal{A} is a modulation-dependent parameter.

Considering the u -th user, the improper integral in (25) can be expressed in terms of the limit when τ approaches infinity, i.e.,

$$P_{b,u} = \frac{1}{2} \lim_{\tau \rightarrow \infty} \int_0^{\tau} \text{erfc} \left(\sqrt{\frac{\mathcal{A} \beta_u \rho \psi_u^2}{N + \rho \psi_u^2 \vartheta_u}} \right) f_{\Psi_u}(\psi_u) d\psi_u. \quad (26)$$

Replacing (13) in (26) and then changing the order of integration, we get

$$P_{b,u} = \frac{k^{NM+1}}{2} \left(\frac{1}{\lambda}\right)^{kNM} \sum_{i=0}^{\infty} \xi_i (i+NM) \times \lim_{\tau \rightarrow \infty} \int_0^{\tau} \text{erfc} \left(\sqrt{\frac{\mathcal{A} \beta_u \rho \psi_u^2}{N + \rho \psi_u^2 \vartheta_u}} \right) \psi_u^{k(i+NM)-1} d\psi_u. \quad (27)$$

Finally, integrating by parts and after some algebraic manipulations with the aid of [32, eq. (4.2.1)], the ABER for the u -th user can be obtained as

$$P_{b,u} = \frac{k^{MN}}{2\lambda^{kMN}} \sum_{i=0}^{\infty} \xi_i \lim_{\tau \rightarrow \infty} \left[\tau^{k(i+MN)} \left(\text{erfc}(\zeta(\tau)) + \frac{2\zeta(i,\tau)}{\sqrt{\pi}} \right) \right], \quad (28)$$

where $\zeta(\tau)$ and $\zeta(i,\tau)$ are auxiliary functions given by

$$\zeta(\tau) = \sqrt{\frac{\mathcal{A} \rho \tau^2 \beta_u}{N + \rho \tau^2 \vartheta_u}} \quad (29)$$

$$\zeta(i,\tau) = \sum_{j=0}^{\infty} \frac{\tau^{2j+1}}{j! (\varepsilon(i,j) + 1)} \left(-\sqrt{\frac{\mathcal{A} \rho \beta_u}{N}} \right)^j \times {}_2F_1 \left(j + \frac{3}{2}, \frac{\varepsilon(i,j) + 1}{2}; \frac{\varepsilon(i,j) + 3}{2}; -\frac{\tau^2 \vartheta_u}{N \rho^{-1}} \right), \quad (30)$$

in which $\varepsilon(i,j) = 2j + ik + kMN$ and ${}_2F_1(\cdot, \cdot; \cdot; \cdot)$ is the Gauss hypergeometric function [34, Eq. (15.1.1)].

To ease the numerical calculation, (28) can be accurately approximated as

$$P_{b,u} \approx \frac{k^{MN}}{2\lambda^{kMN}} \sum_{i=0}^{\infty} \xi_i (a^\dagger)^{k(i+MN)} \left(\text{erfc}(\zeta_{(a^\dagger)}) + \frac{2\zeta_{(i,a^\dagger)}}{\sqrt{\pi}} \right), \quad (31)$$

where a^\dagger is an accuracy-dependent parameter. The higher the values of a^\dagger , the higher the accuracy. A value of $a^\dagger = 35$ guarantees a relative error of less than 10^{-6} , as will be seen in Section V.

Following the same derivation steps as in (28), the exact ABER for the first user can be obtained as

$$P_{b,1} = \frac{k^{MN}}{2\sqrt{\pi}\lambda^{kMN}} \times \sum_{i=0}^{\infty} \xi_i \Gamma \left(\frac{ik + kMN + 1}{2} \right) \left(\frac{N}{\mathcal{A} \beta_1 \rho} \right)^{\frac{k}{2}(i+MN)}. \quad (32)$$

An asymptotic ABER for the first user can also be found by using the first term in (32), resulting in

$$P_{b,1} \simeq (G_{c,1} \rho)^{-G_{d,1}}, \quad (33)$$

where $G_{d,1} = kMN/2$ is the diversity gain and

$$G_{c,1} = \frac{\mathcal{A} \beta_1 \lambda^2}{N} \left[\left(\frac{\Gamma(\frac{kMN+1}{2})}{2\sqrt{\pi}} \right)^M \frac{\Gamma(k+1)^N}{\Gamma(kN+1)} \right]^{-\frac{2}{kN}} \quad (34)$$

is the coding gain.

It is important to highlight that all exact expressions derived herein converge rapidly (i.e., with few summation terms) and are new in the literature.

1) *Minimum Achievable ABER for the u -th user:* Using a partial fraction decomposition into (3b), we obtain

$$\chi_u = \frac{\mathcal{A} \beta_u}{\vartheta_u} - \frac{\mathcal{A} N \beta_u}{\vartheta_u (N + \rho \Psi^2 \vartheta_u)}. \quad (35)$$

Noticing that in the high SNR regime (i.e., when $\rho \rightarrow \infty$), the second term vanishes. Then, an asymptotic expression for the SNR can be obtained as

$$\chi_u \simeq \frac{\mathcal{A} \beta_u}{\vartheta_u}. \quad (36)$$

Finally, substituting (36) into (25), a minimum achievable ABER (i.e., a performance floor at high SNR) for the u -th user can be found as

$$P_{b,u}^{\min} = \frac{1}{2} \text{erfc} \left(\sqrt{\frac{\mathcal{A} \beta_u}{\vartheta_u}} \right). \quad (37)$$

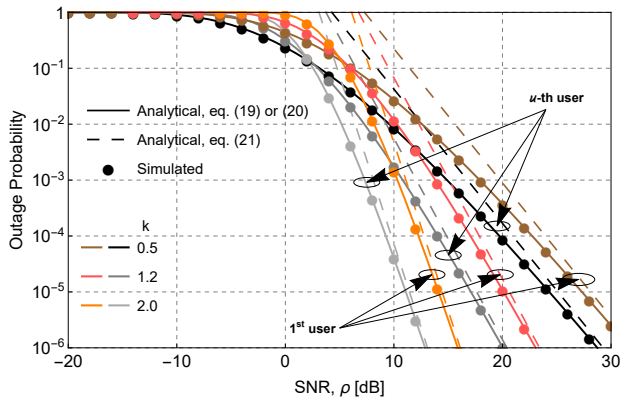


Fig. 2. OP versus SNR using $\lambda = 2$, $N = 2$, $M = 3$, $\gamma_u = 0$, $\beta_u = 0.55$, $\beta_1 = 0.01$, $\vartheta_u = 0.45$, and various values of k .

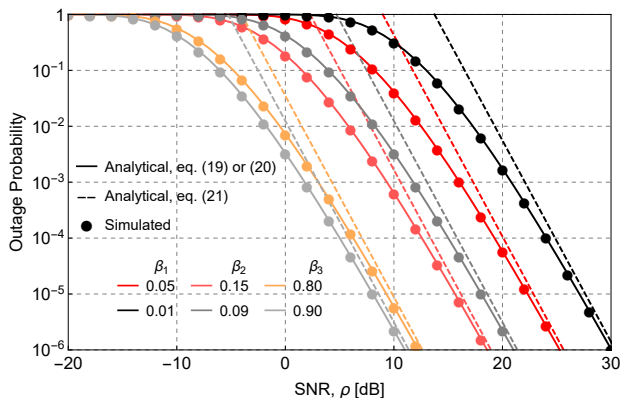


Fig. 3. OP versus SNR using $k = 1.2$, $N = 2$, $M = 3$, $\gamma_u = 0$, and various values of β_u . This corresponds to two scenarios with three users each and with different allocation of power coefficients.

Notice that the minimum achievable ABER for the u -th user is independent of the channel statistics (e.g., the type of fading) and on the number of antennas in the diversity schemes (e.g., EGC, MRC, and TAS). Indeed, it only depends on the user's power allocation coefficient and the type of modulation.

V. NUMERICAL RESULTS

In this section, we corroborate our analytical findings through Monte-Carlo simulations.²

Figs. 2 and 3 show the OPs in terms of the SNR varying the values of k and β_u (which implies varying ϑ_u). In both figures, observe how the system performance improves as k or β_u increases. That is also true when either N or M increases (omitted here due to space limitations). This occurs since the system's diversity order equals $(kNM)/2$. Notice the perfect agreement between Monte-Carlo simulations and our analytical results, thereby corroborating our findings. Moreover, notice how our asymptotic formulations provide good fits in the high-SNR regime.

²The number of Monte-Carlo realizations was set to 10^7 . Also, we used a maximum of 200 terms in our series expressions.

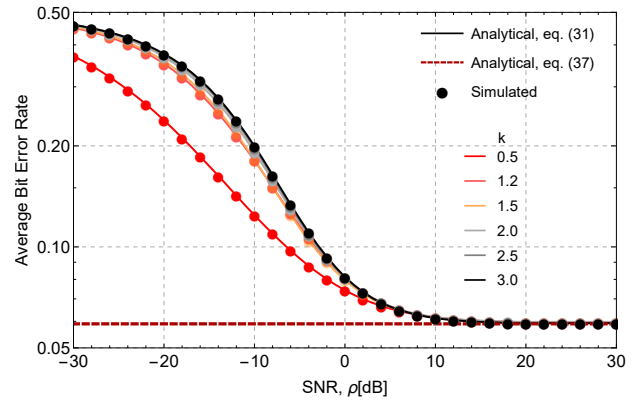


Fig. 4. ABER versus SNR using $N = 2$, $M = 3$, $\mathcal{A} = 1$, $\beta_u = 0.55$, $\vartheta_u = 0.45$ and various values of k .

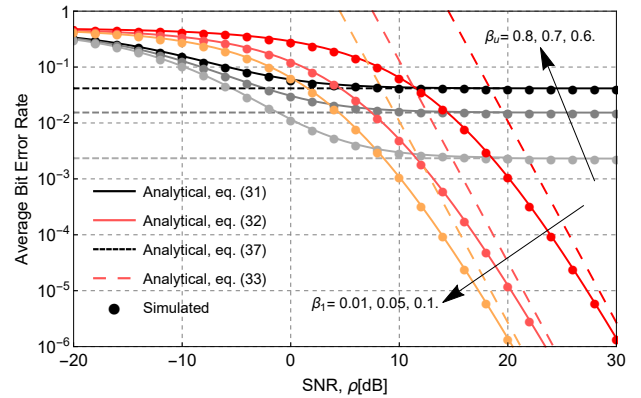


Fig. 5. ABER versus SNR using $k = 1.2$, $N = 2$, $M = 3$, $\mathcal{A} = 1$, $\vartheta_u = 1 - \beta_u$ and various values of β_u and β_1 .

Fig. 4 depicts the ABER for different values of k . Notice that regardless of the values of k , at high SNR the ABER reaches the same minimum value (performance floor), given in (37). (The same occurs for different values of the scale parameter λ , omitted here due to space constraints.) That is, the minimum ABER is independent of the fading parameters.

Finally, Fig. 5 shows the ABERs for different values of β_u and β_1 . It exhibits the different behaviors of both scenarios. For the first user (in red scale), as the SNR increases, the ABER decreases. On the other hand, for the u -th user (in grey scale), the ABER does not fall below a certain performance floor that depends on the value of the power coefficient. The higher the power coefficient, the smaller the minimum ABER. Notice the perfect match between our analytical results and the simulations. Moreover, notice the good fit that our asymptotic formulations provide in the high-SNR regime.

VI. CONCLUSION

This work analyzed the performance of a MIMO-NOMA system operating over Weibull fading channels. Exact formulations for the SNR's statistics, OP, and ABER were provided. An asymptotic analysis was also carried out to show how the physical parameters roughly affect the system performance.

Analytical and numerical results indicate that the system performance improves as k , M , or N increases. Moreover, it was shown that the minimum achievable ABER for the u -th user is independent of the fading scenario and of the number of antennas in the diversity schemes. In fact, it only depends on the user's power allocation coefficient and the type of modulation.

REFERENCES

- [1] Y. L. Lee, D. Qin, L.-C. Wang, and G. H. Sim, "6G massive radio access networks: Key applications, requirements and challenges," *IEEE Open J. Veh. Technol.*, vol. 2, pp. 54–66, Dec. 2021.
- [2] M. Aldababsa, M. Toka, S. Gökçeli, G. K. Kurt, and O. Kucur, "A tutorial on nonorthogonal multiple access for 5G and beyond," *Wireless Communications and Mobile Computing*, vol. 2018, 2018.
- [3] S. M. R. Islam, N. Avazov, O. A. Dobre, and K.-s. Kwak, "Power-domain non-orthogonal multiple access (NOMA) in 5G systems: Potentials and challenges," *IEEE Commun. Surveys Tuts.*, vol. 19, no. 2, pp. 721–742, Oct. 2017.
- [4] K. Yang, N. Yang, N. Ye, M. Jia, Z. Gao, and R. Fan, "Non-orthogonal multiple access: Achieving sustainable future radio access," *IEEE Commun. Mag.*, vol. 57, no. 2, pp. 116–121, Nov. 2019.
- [5] M. Amjad and L. Musavian, "Performance analysis of NOMA for ultra-reliable and low-latency communications," in *IEEE Globecom Workshops (GC Workshops)*, Feb. 2018, pp. 1–5.
- [6] R. Rai, H. Zhu, and J. Wang, "Performance analysis of NOMA enabled fog radio access networks," *IEEE Trans. Commun.*, vol. 69, no. 1, pp. 382–397, Oct. 2021.
- [7] S. Mounchili and S. Hamouda, "Pairing distance resolution and power control for massive connectivity improvement in NOMA systems," *IEEE Trans. Veh. Technol.*, vol. 69, no. 4, pp. 4093–4103, Feb. 2020.
- [8] C. B. Mwakwata, O. Elgarhy, M. M. Alam, Y. Le Moullec, S. Päränd, K. Trichias, and K. Ramantas, "Cooperative scheduler to enhance massive connectivity in 5G and Beyond by minimizing interference in OMA and NOMA," *IEEE Syst. J.*, pp. 1–12, Oct. 2021.
- [9] J. Cheon and H.-S. Cho, "Power allocation scheme for non-orthogonal multiple access in underwater acoustic communications," *Sensors*, vol. 17, no. 11, 2017.
- [10] Z. Chen, Z. Ding, X. Dai, and R. Zhang, "An optimization perspective of the superiority of NOMA compared to conventional OMA," *IEEE Trans. Signal Process.*, vol. 65, no. 19, pp. 5191–5202, Jul. 2017.
- [11] Z. Ding, Y. Liu, J. Choi, Q. Sun, M. Elkashlan, I. Chih-Lin, and H. V. Poor, "Application of non-orthogonal multiple access in LTE and 5G networks," *IEEE Commun. Mag.*, vol. 55, no. 2, pp. 185–191, Feb. 2017.
- [12] P. Sharma, A. Kumar, and M. Bansal, "Performance analysis of downlink NOMA over $\eta - \mu$ and $\kappa - \mu$ fading channels," *IET Communications*, vol. 14, no. 3, pp. 522–531, 2020.
- [13] —, "On performance of downlink NOMA with equal gain combining over $\kappa - \mu$ fading channel for limiting value of κ ," in *Proc. IEEE 4th Conf. Inf. Commun. Technol. (CICT)*, Dec. 2020, pp. 1–6.
- [14] —, "Performance analysis of downlink NOMA system with diversity combining schemes over $\eta - \mu$ fading channel," *Phys. Commun.*, vol. 47, p. 101383, 2021.
- [15] A. P. Shrestha, T. Han, Z. Bai, J. M. Kim, and K. S. Kwak, "Performance of transmit antenna selection in non-orthogonal multiple access for 5G systems," in *Proc. 8th Int. Conf. Ubiquitous Future Ntw.*, Jul. 2016, pp. 1031–1034.
- [16] N.-L. Nguyen, H.-N. Nguyen, N.-T. Nguyen, D.-T. Do, A.-T. Le, M. Voznak, and J. Zdralek, "On secure cognitive radio networks with NOMA: Design of multiple-antenna and performance analysis," in *Proc. IEEE Microw. Theory Techn. Wireless Commun.*, vol. 1, Nov. 2020, pp. 1–6.
- [17] M. Aldababsa and O. Kucur, "Outage performance of NOMA with majority based TAS/MRC scheme in Rayleigh fading channels," in *Proc. 27th Signal Process. Commun. Appl. Conf. (SIU)*, Aug. 2019, pp. 1–4.
- [18] A. Alqahtani, E. Alsusa, A. Al-Dweik, and M. Al-Jarrah, "Performance analysis for downlink NOMA over $\alpha - \mu$ generalized fading channels," *IEEE Trans. Veh. Technol.*, vol. 70, no. 7, pp. 6814–6825, May 2021.
- [19] B. M. ElHalawany, F. Jameel, D. B. da Costa, U. S. Dias, and K. Wu, "Performance analysis of downlink NOMA systems over $\kappa - \mu$ shadowed fading channels," *IEEE Trans. Veh. Technol.*, vol. 69, no. 1, pp. 1046–1050, Jan. 2021.
- [20] N. Jaiswal and N. Purohit, "Performance analysis of NOMA-enabled vehicular communication systems with transmit antenna selection over double Nakagami- m fading," *IEEE Trans. Veh. Technol.*, vol. 70, no. 12, pp. 12 725–12 741, Dec. 2021.
- [21] D. G. Brennan, "Linear diversity combining techniques," *Proc. IRE*, vol. 47, pp. 1075–1102, Jun. 1959.
- [22] N. C. Beaulieu, "An infinite series for the computation of the complementary probability distribution function of a sum of independent random variables and its application to the sum of Rayleigh random variables," *IEEE Trans. Commun.*, vol. 38, no. 9, pp. 1463–1474, Sep. 1990.
- [23] G. Karagiannidis, D. Zogas, N. Sagias, S. Kotsopoulos, and G. Tombras, "Equal-gain and maximal-ratio combining over nonidentical Weibull fading channels," *IEEE Trans. Wireless Commun.*, vol. 4, no. 3, pp. 841–846, May 2005.
- [24] M. Ismail and M. Matalgah, "Performance of dual maximal ratio combining diversity in nonidentical correlated Weibull fading channels using Pade/spl acute/ approximation," *IEEE Tran. Commun.*, vol. 54, no. 3, pp. 397–402, Mar. 2006.
- [25] T. Chaayra, F. E. Bouanani, and H. Ben-azza, "Performance analysis of TAS/MRC based mimo systems over Weibull fading channels," in *Proc. Int. Conf. Advanced Commun. Syst. Inf. Security (ACOSIS)*, Feb. 2016, pp. 1–6.
- [26] M. Bilim, "Approximate ASER analysis of MIMO TAS/MRC networks over Weibull fading channels," *Ann. Telecommun.*, vol. 76, no. 1, pp. 73–81, 2021.
- [27] Q. T. Zhang, "Error rates for 4-branch equal-gain combining in independent Rayleigh fading: A simple explicit solution," *IEEE Commun. Lett.*, vol. 26, no. 2, pp. 269–272, Feb. 2022.
- [28] J. Liberti, S. Moshavi, and P. Zablocky, "Successive interference cancellation," *US Patent 8670418 B*, vol. 2, 2014.
- [29] T. Hou, X. Sun, and Z. Song, "Outage performance for non-orthogonal multiple access with fixed power allocation over Nakagami- m fading channels," *IEEE Commun. Lett.*, vol. 22, no. 4, pp. 744–747, Apr. 2018.
- [30] J. M. Moualeu, D. B. da Costa, F. J. Lopez-Martinez, W. Hamouda, T. M. N. Nkouatchah, and U. S. Dias, "Transmit antenna selection in secure MIMO systems over $\alpha - \mu$ fading channels," *IEEE Trans. Commun.*, vol. 67, no. 9, pp. 6483–6498, Sep. 2019.
- [31] F. D. A. García, F. R. A. Parente, G. Fraidenaich, and J. C. S. S. Filho, "Light exact expressions for the sum of Weibull random variables," *IEEE Wireless Commun. Lett.*, vol. 10, no. 11, pp. 2445–2449, Nov. 2021.
- [32] M. Abramowitz and I. A. Stegun, *Handbook of Mathematical Functions with Formulas, Graphs, and Mathematical Tables*, 10th ed. Washington, DC: US Dept. of Commerce: National Bureau of Standards, 1972.
- [33] M. K. Simon and M.-S. Alouini, *Digital communication over fading channels*, 2nd ed. Hoboken: NJ: Wiley, 2004.
- [34] F. W. J. Olver, D. W. Lozier, R. F. Boisvert, and C. W. Clark, *NIST Handbook of Mathematical Functions*, 1st ed. Washington, DC: US Dept. of Commerce: National Institute of Standards and Technology (NIST), 2010.